

Investigation of the isotopic dependence in the synthesis of superheavy nuclei with Plutonium and Curium targets*

Ming-Hao Zhang,^{1,2} Mei-Chen Wang,^{1,2} Ying Zou,^{1,2} Gen Zhang,³ Qing-Lin Niu,^{1,2} and Feng-Shou Zhang^{1,2,4,†}

¹The Key Laboratory of Beam Technology of Ministry of Education,

School of Physics and Astronomy, Beijing Normal University, Beijing 100875, China

²Institute of Radiation Technology, Beijing Academy of Science and Technology, Beijing 100875, China

³School of Physical Science and Technology, Guangxi University, Nanning 530004, China

⁴Center of Theoretical Nuclear Physics, National Laboratory of Heavy Ion Accelerator of Lanzhou, Lanzhou 730000, China

In the synthesis of new superheavy nuclei, the various long half-lives of Pu and Cm isotopes render them promising as target materials for the fusion reactions. An investigation into the isotopic dependence of the actinide targets is important to select optimal reaction systems. Based on the dinuclear system model, the influential factors on the isotopic dependence are investigated for the reactions $^{48}\text{Ca}+^{239,240,242,244}\text{Pu}$. The reaction systems with the $^{242-248}\text{Cm}$ targets and the ^{45}Sc , ^{50}Ti , ^{51}V , ^{54}Cr , ^{55}Mn projectiles are investigated for the synthesis of new isotopes $^{284-290}\text{Ts}$, $^{289-293,295}\text{Og}$, $^{290-296}\text{119}$, $^{293-299}\text{120}$, $^{294-300}\text{121}$. The isotopic dependence of the Cm targets reveals an ascending trend of the maximal ER cross section coupled with an odd-even effect as the neutron number of the target increases, and the ^{247}Cm target emerges promising in future experiments. The optimal reactions for producing new superheavy elements with $Z = 119-121$ are predicted to be the reactions $^{51}\text{V}+^{245}\text{Cm}$, $^{54}\text{Cr}+^{247}\text{Cm}$ and $^{55}\text{Mn}+^{247}\text{Cm}$ with the maximal ER cross sections of 144 fb, 0.877 fb and 0.052 fb, respectively.

Keywords: Superheavy nuclei, Dinuclear system model, Fusion reaction, Isotopic dependence

I. INTRODUCTION

The synthesis and investigation of unknown superheavy elements (SHEs) can reveal the shell structure and decay properties near the predicted "island of stability" [1–4]. Over recent decades, remarkable advancements have been achieved in the synthesis of new SHEs with $Z = 114-118$ through fusion reactions with the ^{48}Ca projectile and the actinide targets [5–9]. To date, modern accelerators coupled with sensitive detection techniques have made notable progress in the synthesis of new superheavy nuclei [10–17]. Despite these advances, a significant gap remains unfilled in the superheavy nuclei region, necessitating continued experimental and theoretical investigations.

For synthesizing new superheavy nuclei, the ^{48}Ca -induced fusion reactions encounter constraints due to the limited amount of experimental feasible Bk and Cf targets. Consequently, employing combinations of Cm targets and heavier stable projectiles can be alternatives for future experiments. The mixed-Cm target material was produced via irradiation of Plutonium target in the Savannah River Site, with subsequent recovery at the Oak Ridge National Laboratory [18]. With long half-lives ranging from decades to millions of years, many Pu and Cm isotopes have been extensively applied as target materials in fusion reactions aimed at synthesizing new isotopes [12, 19–34]. In 2022, the reaction $^{51}\text{V}+^{248}\text{Cm}$ was tried to synthesize the new element with $Z = 119$, and the

optimal reaction energy for this reaction was estimated [35]. These experiments reveal the critical influence of the target neutron excess on the maximal ER cross sections, indicating the necessity for further research into the isotopic dependence of target materials.

Based on the experimental results, a variety of theoretical models, including both the macroscopic [36–41] and the microscopic approaches [42–49], have been developed. Among these, the dinuclear system (DNS) model has been proven to be reliable in investigating the fusion-evaporation reactions [50–63]. Within the framework of the DNS model, the fusion-evaporation process is divided into three stages: initial formation of the DNS upon overcoming the Coulomb barrier by the colliding nuclei; subsequent production of a compound nucleus through nucleon transfer from the lighter projectile to the heavier target; and finally, the synthesis of a superheavy nucleus via evaporating neutrons by the excited compound nucleus to reach the ground state.

Experiments reveal that the evaporation residual (ER) cross sections of the fusion reactions exhibit remarkable sensitivity to the selection of target material [12, 64]. The isotopic dependence of target not only affects the ER cross sections of synthesizing new superheavy nuclei, but also influences their decay properties and the feasibility of observation for a sufficient duration to study their chemical and physical properties. As a result, to search for the optimal projectile-target combinations, it is necessary to investigate the isotopic dependence of target materials. Based on the DNS model, this paper discusses the isotopic dependence of the targets and investigates the potential for extending the superheavy nuclei region with Cm targets.

This article is organized as follows: In Sec. II, we describe the theoretical framework of the DNS model. In Sec. III, the reliability of the DNS model has been examined based on the ample experimental results of the fusion reactions

* Supported by the National Key R&D Program of China under Grant No. 2023YFA1606401, the National Natural Science Foundation of China under Grants No.12135004, No.11635003 and No.11961141004 and the Guangxi Natural Science Foundation under Grant No.2022GXNSFBA035549.

† Corresponding author, fszhang@bnu.edu.cn

$^{48}\text{Ca}+^{239,240,242,244}\text{Pu}$, with an investigation into the influential factors of the isotopic dependence. Additionally, the experimental results of the reactions $^{48}\text{Ca}+^{245,248}\text{Cm}$ are compared with the theoretical calculations. The combinations of the $^{242-248}\text{Cm}$ target and the ^{45}Sc , ^{50}Ti , ^{51}V , ^{54}Cr and ^{55}Mn projectiles are investigated for extending the superheavy nuclei region with $Z = 117-121$, presenting the maximal ER cross sections and corresponding incident energies. The isotopic dependence of the Cm targets has been discussed in the capture, fusion and survival stages in detail. In Sec. IV, a summary of this work is provided.

II. THEORETICAL DESCRIPTIONS

Within the framework of the DNS model, the ER cross section as a function of the center-of-mass energy $E_{\text{c.m.}}$ is calculated by summing over the contributing partial waves J :

$$\sigma_{\text{ER}}(E_{\text{c.m.}}) = \frac{\pi \hbar^2}{2\mu E_{\text{c.m.}}} \sum_J (2J+1) T(E_{\text{c.m.}}, J) \times P_{\text{CN}}(E_{\text{c.m.}}, J) W_{\text{sur}}(E_{\text{c.m.}}, J), \quad (1)$$

In this formula, $T(E_{\text{c.m.}}, J)$ is the transmission probability for forming the dinuclear system. $P_{\text{CN}}(E_{\text{c.m.}}, J)$ denotes the probability of complete fusion into a compound nucleus [65]. $W_{\text{sur}}(E_{\text{c.m.}}, J)$ represents the probability that the excited compound nucleus survives against fission [66]. The interaction potential of the colliding nuclei is given as [67]:

$$V(R, \beta_1, \beta_2, \theta_1, \theta_2) = \frac{1}{2} C_1 (\beta_1 - \beta_1^0)^2 + \frac{1}{2} C_2 (\beta_2 - \beta_2^0)^2 + V_{\text{C}}(R, \beta_1, \beta_2, \theta_1, \theta_2) + V_{\text{N}}(R, \beta_1, \beta_2, \theta_1, \theta_2). \quad (2)$$

Here $C_{1,2}$ denotes the stiffness of the nuclear surface predicted by the liquid drop model [68]. The deformation parameters $\beta_{1,2}$ represent the dynamic quadrupole deformations of the projectile and target nucleus, while $\beta_{1,2}^0$ indicate their static deformations. V_{C} is the Coulomb potential calculated via Wong formula [69]. V_{N} denotes the nuclear potential given by the double-folding potential [70].

The transmission probability that represents the capacity of colliding nuclei to surpass the Coulomb barrier is determined as:

$$T(E_{\text{c.m.}}, J) = \int f(B) T(E_{\text{c.m.}}, B, J) dB. \quad (3)$$

$T(E_{\text{c.m.}}, B, J)$ is given by the Ahmed formula [71–73]. The barrier distribution $f(B)$ is taken as an asymmetric Gaussian function with the parameters given in Ref. [74]. The capture cross section σ_{cap} is presented as follows [67]:

$$\sigma_{\text{cap}}(E_{\text{c.m.}}) = \frac{\pi \hbar^2}{2\mu E_{\text{c.m.}}} \sum_J (2J+1) T(E_{\text{c.m.}}, J). \quad (4)$$

In the DNS model, it is assumed that the two touching nuclei maintain their individual identities along with their ground state characteristics and deformations. The fusion mechanism is considered as a diffusion process along the mass asymmetry degree $\eta = (A_1 - A_2)/(A_1 + A_2)$. The nucleon transfer process with the dissipation of the kinetic energy and angular momentum occurs at the valley of the potential energy surface defined as the driving potential [67]. To form a compound nucleus, the dinuclear system must possess sufficient energy to overcome the inner fusion barrier B_{fus} , which is the energy difference between the incident point and the point of maximum driving potential (B.G. point). Therefore, with the interaction time $\tau_{\text{int}}(J)$ given by the deflection function method [75], the fusion probability is obtained by the summation of the distribution probabilities of the fragments that successfully overcome the inner fusion barrier:

$$P_{\text{CN}}(E_{\text{c.m.}}, J) = \sum_{Z_1=1}^{Z_{\text{B.G.}}} \sum_{N_1=1}^{N_{\text{B.G.}}} P(Z_1, N_1, E_1, \tau_{\text{int}}(J)), \quad (5)$$

Here the distribution probability $P(Z_1, N_1, E_1, t)$ is determined through the resolution of a set of two-dimensional master equations [76]:

$$\begin{aligned} \frac{dP(Z_1, N_1, E_1, t)}{dt} &= \sum_{Z'_1} W_{Z_1, N_1; Z'_1, N_1}(t) \\ &\times [d_{Z_1, N_1} P(Z'_1, N_1, E_1, t) - d_{Z'_1, N_1} P(Z_1, N_1, E_1, t)] \\ &+ \sum_{N'_1} W_{Z_1, N_1; Z_1, N'_1}(t) \\ &\times [d_{Z_1, N_1} P(Z_1, N'_1, E_1, t) - d_{Z_1, N'_1} P(Z_1, N_1, E_1, t)] \\ &- [\Lambda_{\text{qf}}(\Theta(t)) + \Lambda_{\text{fis}}(\Theta(t))] P(Z_1, N_1, E_1, t). \end{aligned} \quad (6)$$

$W_{Z_1, N_1; Z'_1, N_1}$ denotes the mean transition probability from (Z_1, N_1) to (Z'_1, N_1) [77], d_{Z_1, N_1} is the microscopic dimension associated with (Z_1, N_1) . Λ_{qf} and Λ_{fis} represent the quasi-fission and fission probability obtained via the one-dimensional Kramers formula [78].

For the evaporation of x neutrons, the survival probability is given by the statistical model:

$$W_{\text{sur}}(E_{\text{CN}}^*, x, J) = P(E_{\text{CN}}^*, x, J) \prod_{i=1}^x \left[\frac{\Gamma_{\text{n}}(E_i^*, J)}{\Gamma_{\text{n}}(E_i^*, J) + \Gamma_{\text{f}}(E_i^*, J)} \right]. \quad (7)$$

$P(E_{\text{CN}}^*, x, J)$ is the realization probability of emitting x neutrons at excitation energy E_{CN}^* [79]. E_i^* denotes the excitation energy before evaporating the i -th neutron. The partial decay width for neutron evaporation Γ_{n} and the fission decay width Γ_{f} are determined employing the Weisskopf-Ewing theory [80] and the Bohr-Wheeler transition-state method [81], respectively. In the calculation of Γ_{f} , the fission barrier of the rotating nucleus is expressed as:

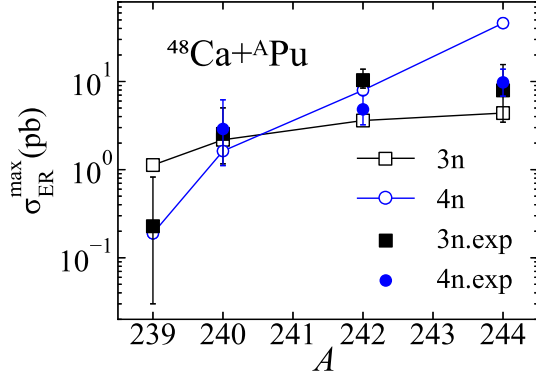


Fig. 1. (Color online) The experimental [19–24, 31, 32] and calculated maximal ER cross sections in the 3n and 4n-emission channel of the reactions $^{48}\text{Ca}+^{239,240,242,244}\text{Pu} \rightarrow ^{287,288,290,292-xn}\text{Fl}+xn$.

$$B_f(E^*, J) = B_f^{\text{LD}}(1 - x_{\text{LD}}T_i^2) + B_f^{\text{M}}(E^* = 0, J) \exp\left(-\frac{E^*}{E_D}\right) - \left(\frac{\hbar^2}{2J_{\text{g.s.}}} - \frac{\hbar^2}{2J_{\text{s.d.}}}\right) J(J+1), \quad (8)$$

Here, B_f^{LD} denotes the macroscopic part determined by the liquid-drop model. B_f^{M} is the microscopic shell correction [1]. x_{LD} and E_D represent the temperature dependent parameter and the shell damping energy, respectively, as defined in Ref. [82]. $J_{\text{g.s.}}$ and $J_{\text{s.d.}}$ are the moments of inertia of the compound nucleus in the ground state and at the saddle point, respectively [83, 84]. In this work we analyze uncertainties arise from the parameterized E_D [56, 85, 86].

III. RESULTS AND DISCUSSION

A. The isotopic dependence of the reactions with $^{239,240,242,244}\text{Pu}$ targets

Given the large amount of available experimental data, the Pu-based hot fusion reactions stand as a crucial assessment for theoretical models. Typically, a higher neutron excess in the target leads to an enhanced maximal ER cross section. Fig. 1 presents both experimental and theoretical maximal ER cross sections of the 3n- and 4n-emission channels for the reactions $^{48}\text{Ca}+^{239,240,242,244}\text{Pu}$. An ascending trend is observed in both experimental and theoretical maximal ER cross sections with the growing neutron number in the target. Notably, the maximal ER cross sections of the 4n-emission channel increase more rapidly compared to those of the 3n-emission channel as the neutron number of the target rises. To understand the isotopic dependence of the target, thorough investigations on the capture, fusion and survival stages are required.

Fig. 2(a) presents the capture cross sections of the reactions $^{48}\text{Ca}+^{239,240,242,244}\text{Pu}$ at $E_{\text{CN}}^* = 35, 40$ and 45 MeV.

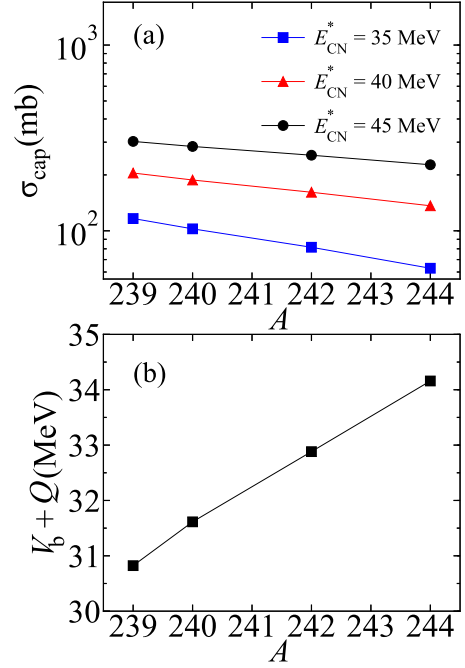


Fig. 2. (Color online) (a) The calculated capture cross sections for the reactions $^{48}\text{Ca}+^{239,240,242,244}\text{Pu} \rightarrow ^{287,288,290,292-xn}\text{Fl}+xn$ with $E_{\text{CN}}^* = 35$ MeV, 40 MeV and 45 MeV. (b) The excitation energies of the corresponding Coulomb barriers of the reactions $^{48}\text{Ca}+^{239,240,242,244}\text{Pu} \rightarrow ^{287,288,290,292-xn}\text{Fl}+xn$.

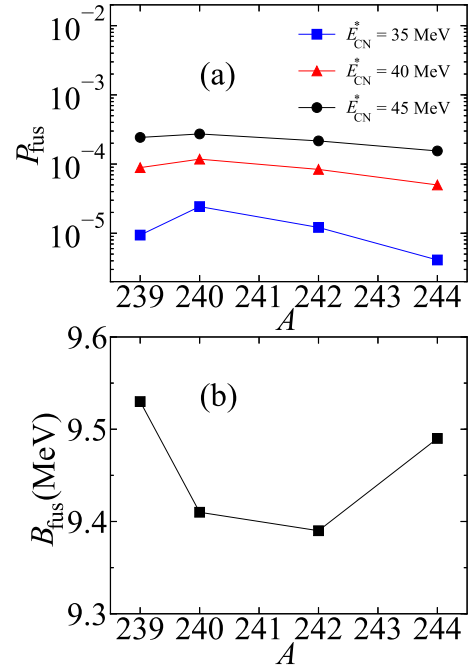


Fig. 3. (Color online) (a) The calculated fusion probabilities for the reactions $^{48}\text{Ca}+^{239,240,242,244}\text{Pu} \rightarrow ^{287,288,290,292-xn}\text{Fl}+xn$ with $E_{\text{CN}}^* = 35$ MeV, 40 MeV and 45 MeV. (b) The B_{fus} values of the reactions $^{48}\text{Ca}+^{239,240,242,244}\text{Pu} \rightarrow ^{287,288,290,292-xn}\text{Fl}+xn$.

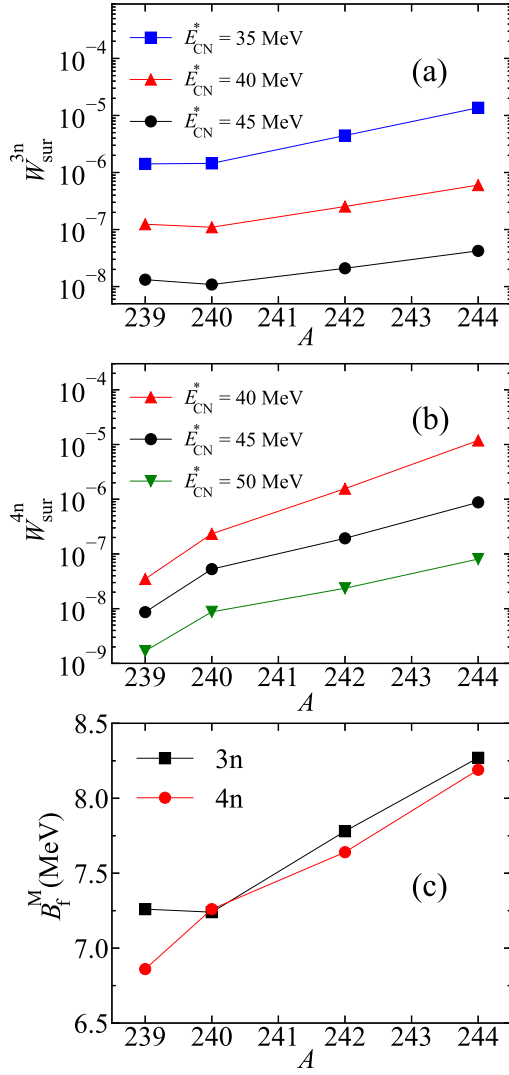


Fig. 4. (Color online) (a) The calculated survival probabilities for the reactions $^{48}\text{Ca}+^{239,240,242,244}\text{Pu} \rightarrow ^{287,288,290,292-xn}\text{Fl}+xn$ with $E_{\text{CN}}^* = 35$ MeV, 40 MeV and 45 MeV. (b) The calculated survival probabilities for the same reactions with $E_{\text{CN}}^* = 40$ MeV, 45 MeV and 50 MeV. (c) The B_f^M values of the corresponding emission channel for the reactions $^{48}\text{Ca}+^{239,240,242,244}\text{Pu} \rightarrow ^{287,288,290,292-xn}\text{Fl}+xn$.

It reveals that the capture cross sections increase with rising E_{CN}^* , due to the enhanced probability at higher E_{CN}^* for the colliding nuclei to overcome the Coulomb barrier. A slight declining trend in the capture cross sections can be observed as the neutron number of the target increases. This can be attributed to the effect of the Coulomb barrier. Fig. 2(b) illustrates the excitation energies associated with the Coulomb barriers V_b+Q for these reactions. It is evident that the V_b+Q values exhibit an upward trend as the neutron number of the target increases, resulting in the aforementioned decreasing trend in the capture cross section.

For the fusion stage, Fig. 3(a) illustrates the fusion probabilities for the reactions $^{48}\text{Ca}+^{239,240,242,244}\text{Pu}$ at $E_{\text{CN}}^* = 35$, 40 and 45 MeV. It is evident that the fusion probabilities ex-

hibit a slight decreasing trend with increasing neutron number of the Pu target. Moreover, as the E_{CN}^* increases, the fusion probabilities are enhanced, and the isotopic effect on the fusion probabilities gradually diminishes. This can be attributed to the influence of the inner fusion barrier. The formation of the compound nucleus requires overcoming the inner fusion barrier, otherwise the quasi-fission occurs. At higher E_{CN}^* , the impediment from the inner fusion barrier fades, leading to higher fusion probability and diminished isotopic dependence. In Fig. 3(b), the inner fusion barrier height B_{fus} values of the Pu-based reactions are presented. The B_{fus} exhibit a slight variation, approximately 0.1 MeV, resulting in the minimal differences in the fusion probabilities, less than an order of magnitude.

Fig. 4(a) and Fig. 4(b) display the survival probabilities of the compound nuclei formed via the reactions $^{48}\text{Ca}+^{239,240,242,244}\text{Pu}$ in the 3n- and 4n-emission channels at different E_{CN}^* . It is observed that as the E_{CN}^* increases, the survival probabilities diminish, suggesting that the compound nucleus becomes less stable and is more likely to undergo fission at high E_{CN}^* . Additionally, both Fig. 4(a) and Fig. 4(b) reveal an enhancement in the survival probabilities with the neutron-rich target. This trend is due to the enhanced stability of the formed compound nucleus as approaching the closed neutron shell.

Notably, the variation among survival probabilities in the 3n-emission channel is about an order of magnitude, yet in the 4n-emission channel, the variation is about two orders of magnitude. This can be attributed to the influence of the fission barrier height B_f^M . Within the DNS model, the survival probability is determined by the competition of fission and neutron emission. In Fig. 4(c), the B_f^M values are presented. It reveals that as the formed compound nucleus approaches the closed neutron shell $N = 184$, the B_f^M value increases, resulting in the suppressed possibility of fission, thereby enhancing the survival probability. The impact of the fission barrier is more pronounced in the calculation of survival probabilities in the 4n-emission channel due to the additional competition between neutron emission and fission. Hence, with an increase in the neutron number of the target nucleus, a more significant enhancement in the survival probability is observed in the 4n-emission channel. The investigation of the capture, fusion and survival stages reveals a substantial enhancement in the survival probabilities of compound nuclei formed by the neutron-rich Pu targets. This enhancement significantly contributes to the observed high ER cross section.

B. The synthesis of new superheavy nuclei with $^{242-248}\text{Cm}$ targets

In Fig. 5, the comparative analysis between calculated and experimental results is extended to the reactions $^{48}\text{Ca}+^{245}\text{Cm} \rightarrow ^{293-xn}\text{Lv}+xn$ and $^{48}\text{Ca}+^{248}\text{Cm} \rightarrow ^{296-xn}\text{Lv}+xn$. It is observed that the theoretical results for both reactions are in agreement with the experimental results in the 3n-emission channel. For the 4n-emission channel, the calculated ER cross sections

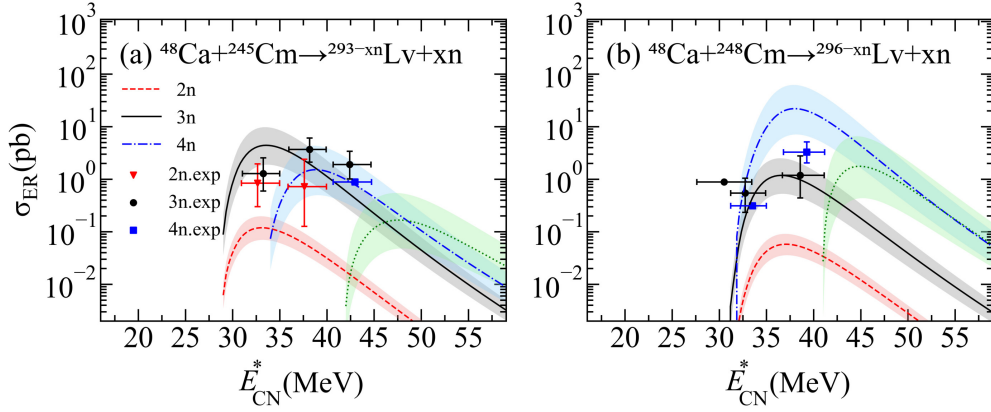


Fig. 5. (Color online) Comparison of the calculated results with the available experimental data of the reactions $^{48}\text{Ca}+^{245,248}\text{Cm} \rightarrow ^{293,296-x}\text{Lv}+x\text{n}$ [5, 31, 32].

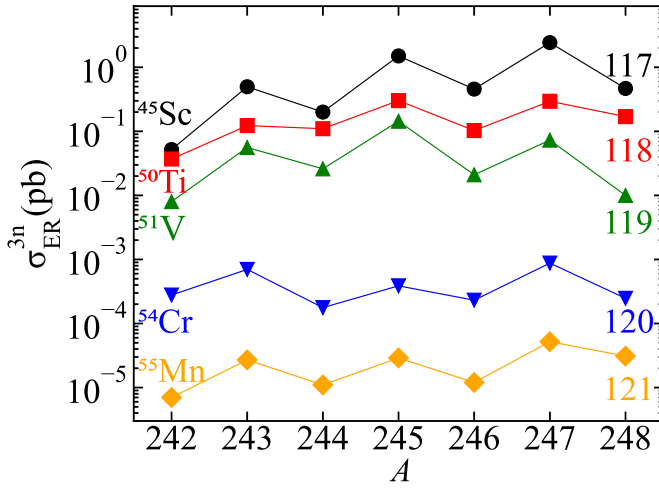


Fig. 6. (Color online) The calculated maximal ER cross sections in the 3n-emission channel for synthesizing new superheavy nuclei with $Z = 117-121$ via the combinations of the ^{45}Sc , ^{50}Ti , ^{51}V , ^{54}Cr and ^{55}Mn projectiles and the $^{242-248}\text{Cm}$ targets.

are consistent with the experimental results for the reaction $^{48}\text{Ca}+^{245}\text{Cm}$, while the calculated maximal ER cross section for the reaction $^{48}\text{Ca}+^{248}\text{Cm}$ exceeds the currently available experimental results. The investigations into the Pu- and Cm-based reactions prove not only the reliability of the DNS model but also its potential in identifying the optimal projectile-target combinations for the synthesis of new superheavy nuclei with Cm targets.

In Table. 1, the optimal reaction systems, alongside the corresponding $E_{c.m.}$, E_{CN}^* and the maximal ER cross sections of the reaction systems with ^{45}Sc , ^{50}Ti , ^{51}V , ^{54}Cr , ^{55}Mn projectiles and $^{242-248}\text{Cm}$ targets are presented. It indicates an exponential decrease in maximal ER cross sections with an increase in the charge number of the formed compound nuclei. The comprehensive analysis of Table. 1 reveals a dominance of the 3n-emission channel in the synthesis of new

superheavy nuclei via the Cm-based reactions. An exception is observed in the synthesis of the isotope ^{293}Og , where the reaction $^{50}\text{Ti}+^{247}\text{Cm} \rightarrow ^{293}\text{Og}+4\text{n}$ exhibits a calculated maximal ER cross section of 114 fb. This value slightly exceeds the maximal ER cross section of 102 fb for the reaction $^{50}\text{Ti}+^{246}\text{Cm} \rightarrow ^{293}\text{Og}+3\text{n}$. For the synthesis of SHE with $Z = 119$, the maximal ER cross section of 144 fb appears in the reaction $^{51}\text{V}+^{245}\text{Cm} \rightarrow ^{293}119+3\text{n}$. However, the synthesis of SHE with $Z = 120$ and 121 exhibits significantly reduced maximal ER cross sections of 0.877 fb for the reaction $^{54}\text{Cr}+^{247}\text{Cm} \rightarrow ^{298}120+3\text{n}$ and 0.052 fb for the reaction $^{55}\text{Mn}+^{247}\text{Cm} \rightarrow ^{299}121+3\text{n}$, respectively, which can be attributed to the increase in the mass number of projectile.

C. The isotopic dependence of the reactions with $^{242-248}\text{Cm}$ targets

To further investigate the isotopic dependence of the $^{242-248}\text{Cm}$ target, the calculated maximal ER cross sections of the Cm-based reactions in the 3n-emission channel are plotted in Fig. 6. A rising trend in the maximal ER cross sections can be observed as the neutron excess in the Cm target increases. This trend is accompanied by an apparent odd-even stagger, indicating the advantage of the neutron-rich Cm targets with odd neutron number. To further discuss this phenomenon, the capture, fusion and survival stages are discussed in Fig. 7.

In Fig. 7(a), the capture cross sections of the reaction systems with ^{45}Sc , ^{50}Ti , ^{51}V , ^{54}Cr , ^{55}Mn projectiles and $^{242-248}\text{Cm}$ targets are presented. Consistent with aforementioned discussion, the capture cross sections display a decreasing trend as the neutron number of the target increases. For ^{45}Sc -induced reactions, the isotopic effect on the capture is relatively significant. For the other reactions, the capture cross section exhibits considerably less variation. Fig. 7(b) presents the fusion probabilities of the corresponding reactions. A significant decline in the fusion probabilities can be observed between the ^{45}Sc - and ^{50}Ti -induced reactions as

TABLE 1. The optimal Cm-based reaction systems for producing new superheavy nuclei with $Z=117-121$. The isotopes, the reaction systems, the optimal incident energy $E_{c.m.}$, the E_{CN}^* and the maximal calculated ER cross sections are listed in columns 1-5, respectively.

| Isotope | Reaction | $E_{c.m.}$ (MeV) | E_{CN}^* (MeV) | σ_{ER}^{max} (fb) |
|--------------------|---------------------------------------|---------------------|---------------------|-----------------------------|
| ^{242}Cm | $(^{45}\text{Sc}, 3n)$ | 209.0 | 38.0 | 52^{+45}_{-25} |
| ^{285}Ts | $^{243}\text{Cm}(^{45}\text{Sc}, 3n)$ | 205.7 | 36.0 | 497^{+465}_{-250} |
| ^{286}Ts | $^{244}\text{Cm}(^{45}\text{Sc}, 3n)$ | 204.6 | 36.0 | 200^{+197}_{-103} |
| ^{287}Ts | $^{245}\text{Cm}(^{45}\text{Sc}, 3n)$ | 202.2 | 35.0 | 1505^{+1554}_{-797} |
| ^{288}Ts | $^{246}\text{Cm}(^{45}\text{Sc}, 3n)$ | 202.0 | 36.0 | 457^{+479}_{-243} |
| ^{289}Ts | $^{247}\text{Cm}(^{45}\text{Sc}, 3n)$ | 199.7 | 35.0 | 2430^{+2641}_{-1318} |
| ^{290}Ts | $^{248}\text{Cm}(^{45}\text{Sc}, 3n)$ | 200.3 | 37.0 | 468^{+508}_{-253} |
| ^{289}Og | $^{242}\text{Cm}(^{50}\text{Ti}, 3n)$ | 226.1 | 36.0 | 37^{+38}_{-20} |
| ^{290}Og | $^{243}\text{Cm}(^{50}\text{Ti}, 3n)$ | 224.3 | 35.0 | 123^{+130}_{-66} |
| ^{291}Og | $^{244}\text{Cm}(^{50}\text{Ti}, 3n)$ | 223.5 | 35.0 | 110^{+120}_{-60} |
| ^{292}Og | $^{245}\text{Cm}(^{50}\text{Ti}, 3n)$ | 221.4 | 34.0 | 302^{+344}_{-167} |
| ^{293}Og | $^{247}\text{Cm}(^{50}\text{Ti}, 4n)$ | 224.8 | 39.0 | 114^{+202}_{-75} |
| ^{295}Og | $^{248}\text{Cm}(^{50}\text{Ti}, 3n)$ | 220.0 | 35.0 | 170^{+191}_{-93} |
| $^{290}\text{119}$ | $^{242}\text{Cm}(^{51}\text{V}, 3n)$ | 237.0 | 36.0 | 8^{+8}_{-4} |
| $^{291}\text{119}$ | $^{243}\text{Cm}(^{51}\text{V}, 3n)$ | 234.9 | 35.0 | 56^{+58}_{-30} |
| $^{292}\text{119}$ | $^{244}\text{Cm}(^{51}\text{V}, 3n)$ | 233.9 | 35.0 | 26^{+27}_{-14} |
| $^{293}\text{119}$ | $^{245}\text{Cm}(^{51}\text{V}, 3n)$ | 230.8 | 33.0 | 144^{+157}_{-79} |
| $^{294}\text{119}$ | $^{246}\text{Cm}(^{51}\text{V}, 3n)$ | 231.7 | 35.0 | 21^{+23}_{-11} |
| $^{295}\text{119}$ | $^{247}\text{Cm}(^{51}\text{V}, 3n)$ | 228.8 | 33.0 | 73^{+80}_{-40} |
| $^{296}\text{119}$ | $^{248}\text{Cm}(^{51}\text{V}, 3n)$ | 230.0 | 35.0 | 10^{+10}_{-5} |
| $^{293}\text{120}$ | $^{242}\text{Cm}(^{54}\text{Cr}, 3n)$ | 248.6 | 37.0 | $0.278^{+0.259}_{-0.139}$ |
| $^{294}\text{120}$ | $^{243}\text{Cm}(^{54}\text{Cr}, 3n)$ | 246.9 | 36.0 | $0.699^{+0.658}_{-0.353}$ |
| $^{295}\text{120}$ | $^{244}\text{Cm}(^{54}\text{Cr}, 3n)$ | 246.7 | 37.0 | $0.177^{+0.166}_{-0.089}$ |
| $^{296}\text{120}$ | $^{245}\text{Cm}(^{54}\text{Cr}, 3n)$ | 245.0 | 36.0 | $0.387^{+0.364}_{-0.195}$ |
| $^{297}\text{120}$ | $^{246}\text{Cm}(^{54}\text{Cr}, 3n)$ | 244.1 | 36.0 | $0.231^{+0.220}_{-0.117}$ |
| $^{298}\text{120}$ | $^{247}\text{Cm}(^{54}\text{Cr}, 3n)$ | 242.3 | 35.0 | $0.877^{+0.821}_{-0.443}$ |
| $^{299}\text{120}$ | $^{248}\text{Cm}(^{54}\text{Cr}, 3n)$ | 242.1 | 34.0 | $0.247^{+0.220}_{-0.120}$ |
| $^{294}\text{121}$ | $^{242}\text{Cm}(^{55}\text{Mn}, 3n)$ | 259.1 | 38.0 | $0.007^{+0.005}_{-0.003}$ |
| $^{295}\text{121}$ | $^{243}\text{Cm}(^{55}\text{Mn}, 3n)$ | 256.9 | 37.0 | $0.027^{+0.022}_{-0.012}$ |
| $^{296}\text{121}$ | $^{244}\text{Cm}(^{55}\text{Mn}, 3n)$ | 255.8 | 37.0 | $0.011^{+0.009}_{-0.005}$ |
| $^{297}\text{121}$ | $^{245}\text{Cm}(^{55}\text{Mn}, 3n)$ | 253.6 | 36.0 | $0.029^{+0.024}_{-0.014}$ |
| $^{298}\text{121}$ | $^{246}\text{Cm}(^{55}\text{Mn}, 3n)$ | 253.7 | 37.0 | $0.012^{+0.010}_{-0.006}$ |
| $^{299}\text{121}$ | $^{247}\text{Cm}(^{55}\text{Mn}, 3n)$ | 251.5 | 36.0 | $0.052^{+0.044}_{-0.025}$ |
| $^{300}\text{121}$ | $^{248}\text{Cm}(^{55}\text{Mn}, 3n)$ | 250.7 | 36.0 | $0.031^{+0.025}_{-0.014}$ |

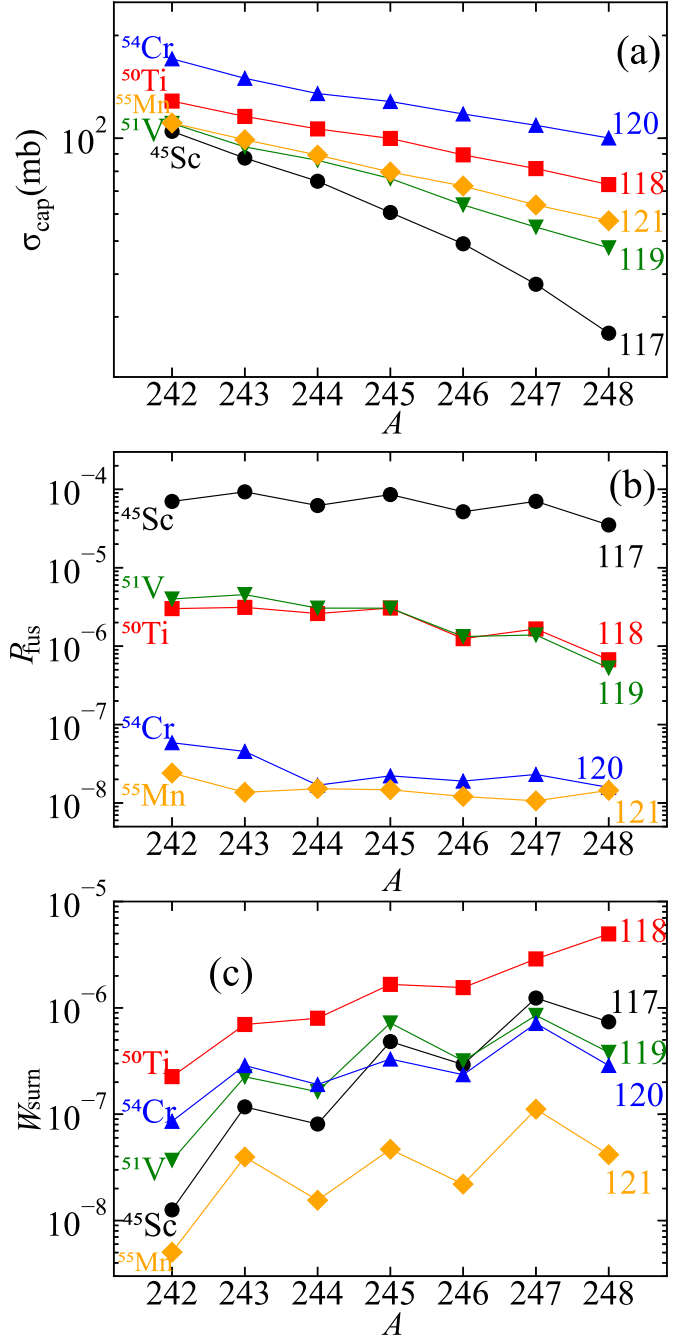


Fig. 7. (Color online) (a) The capture cross sections, (b) the fusion probabilities and (c) the survival probabilities at $E_{CN}^* = 35$ MeV for synthesizing new superheavy nuclei with $Z = 117-121$ via the combinations of the ^{45}Sc , ^{50}Ti , ^{51}V , ^{54}Cr and ^{55}Mn projectiles and the $^{242-248}\text{Cm}$ targets.

well as the ^{51}V - and ^{54}Cr -induced reactions. This can be ascribed to the varying mass asymmetry values influenced by the mass numbers of the projectiles. In Fig. 7(b), a decreasing trend of the fusion probabilities with the rising neutron number of the target can be observed. This isotopic-dependent decreasing trend in fusion probability, along with the same trend discussed in Fig. 3, can be attributed to the deviation in the neutron number of the target from closed neutron shell [87]. Furthermore, an odd-even effect can also be noted, which can be attributed to the pairing effect in the fusion stage.

In Fig. 7(c), the survival probabilities of the corresponding

reactions in the 3n-emission channel are presented. As the neutron number of the formed compound nucleus approaches the predicted closed neutron shell $N = 184$, the stability of the compound nucleus is enhanced, leading to the ascending survival probabilities with rising neutron excess in the target. The odd-even effect is also significant, which primarily comes from the influence of the variance of the fission bar-

rier. It is evident that, in the synthesis of new superheavy nucleus via the $^{242-248}\text{Cm}$ targets, the isotopic dependence on the maximal ER cross section mainly arises from the survival stages. Here, the odd-even effect, coupled with the high neutron excess of the target, strongly enhances the stability of the formed compound nucleus. Consequently, the ^{247}Cm target emerges as favorable in the future synthesis of superheavy nuclei.

IV. SUMMARY

In this paper, the predictive reliability of the DNS model on the isotopic dependence is examined with the experimental results for the reactions $^{48}\text{Ca} + ^{239,240,242,244}\text{Pu}$. The influential factors on the isotopic dependence are discussed in capture, fusion and survival stages, revealing a strong enhancement in the survival probabilities due to the influ-

ence of the fission barrier height. The feasibility of applying the $^{242-248}\text{Cm}$ targets and the stable projectiles ^{45}Sc , ^{50}Ti , ^{51}V , ^{54}Cr , ^{55}Mn for synthesizing new superheavy nuclei $^{284-290}\text{Ts}$, $^{289-293,295}\text{Og}$, $^{290-296}\text{119}$, $^{293-299}\text{120}$, $^{294-300}\text{121}$ is investigated. For synthesizing new superheavy elements with $Z = 119-121$, the optimal reaction systems are predicted to be the reactions $^{51}\text{V} + ^{245}\text{Cm} \rightarrow ^{293}\text{119} + 3\text{n}$, $^{54}\text{Cr} + ^{247}\text{Cm} \rightarrow ^{298}\text{120} + 3\text{n}$ and $^{55}\text{Mn} + ^{247}\text{Cm} \rightarrow ^{299}\text{121} + 3\text{n}$, with the maximal ER cross sections of 144 fb, 0.877 fb and 0.052 fb, respectively. The isotopic dependence on the maximal ER cross sections of the $^{242-248}\text{Cm}$ -based reactions is investigated in detail, indicating that the isotopic dependence of the Cm targets mainly arises from the survival stages. This is attributed to the enhanced stability of the formed compound nuclei, influenced by a higher neutron number when approaching the predicted neutron shell closure $N = 184$. The odd-even effect coupled with the high neutron excess renders the ^{247}Cm target promising in the future synthesis of superheavy nuclei.

-
- [1] P. Möller, A. Sierk, T. Ichikawa et al., Nuclear ground-state masses and deformations: FRDM(2012). *At. Data. Nucl. Data Tables* **109-110**, 1–204 (2016). doi:10.1016/j.adt.2015.10.002
- [2] S. Ćwiok, P. H. Heenen, W. Nazarewicz, Shape coexistence and triaxiality in the superheavy nuclei. *Nature* **433**, 705–709 (2005). doi:10.1038/nature03336
- [3] A. T. Kruppa, M. Bender, W. Nazarewicz et al., Shell corrections of superheavy nuclei in self-consistent calculations. *Phys. Rev. C* **61**, 034313 (2000). doi:10.1103/PhysRevC.61.034313
- [4] D. Ackermann, C. Theisen, Nuclear structure features of very heavy and superheavy nuclei-tracing quantum mechanics towards the ‘island of stability’. *Phys. Scr.* **92** (8), 083002 (2017). doi:10.1088/1402-4896/aa7921
- [5] Y. T. Oganessian, V. K. Utyonkov, Y. V. Lobanov et al., Synthesis of the isotopes of elements 118 and 116 in the ^{249}Cf and $^{245}\text{Cm} + ^{48}\text{Ca}$ fusion reactions. *Phys. Rev. C* **74**, 044602 (2006). doi:10.1103/PhysRevC.74.044602
- [6] Y. T. Oganessian, A. Yeremin, A. Popeko et al., Synthesis of nuclei of the superheavy element 114 in reactions induced by ^{48}Ca . *Nature* **400**, 242 (1999). doi:10.1038/22281
- [7] Y. T. Oganessian, F. S. Abdullin, S. N. Dmitriev et al., Investigation of the $^{243}\text{Am} + ^{48}\text{Ca}$ reaction products previously observed in the experiments on elements 113, 115, and 117. *Phys. Rev. C* **87**, 014302 (2013). doi:10.1103/PhysRevC.87.014302
- [8] Y. T. Oganessian, V. K. Utyonkov, Y. V. Lobanov et al., Observation of the decay of $^{292}\text{116}$. *Phys. Rev. C* **63**, 011301(R) (2000). doi:10.1103/PhysRevC.63.011301
- [9] Y. T. Oganessian, F. S. Abdullin, P. D. Bailey et al., Synthesis of a new element with atomic number $Z = 117$. *Phys. Rev. Lett.* **104**, 142502 (2010). doi:10.1103/PhysRevLett.104.142502
- [10] T. Huang, D. Seweryniak, B. B. Back et al., Discovery of the new isotope ^{251}Lr : Impact of the hexacontetrapole deformation on single-proton orbital energies near the $Z = 100$ deformed shell gap. *Phys. Rev. C* **106**, L061301 (2022). doi:10.1103/PhysRevC.106.L061301
- [11] K. Morita, K. Morimoto, D. Kaji et al., Experiment on the synthesis of element 113 in the reaction $^{209}\text{Bi} (^{70}\text{Zn}, \text{n}) ^{278}\text{113}$. *J. Phys. Soc. Jpn.* **73**, 2593 (2004). doi:10.1143/jpsj.73.2593
- [12] Y. T. Oganessian, V. K. Utyonkov, Super-heavy element research. *Rep. Prog. Phys.* **78** (3), 036301 (2015). doi:10.1088/0034-4885/78/3/036301
- [13] Y. Oganessian, V. Utyonkov, Superheavy nuclei from ^{48}Ca -induced reactions. *Nucl. Phys. A* **944**, 62–98 (2015). doi:10.1016/j.nuclphysa.2015.07.003
- [14] M. Thoennessen, Discovery of isotopes of elements with $Z \geq 100$. *At. Data. Nucl. Data Tables*. **99** (3), 312–344 (2013). doi:10.1016/j.adt.2012.03.003
- [15] Z. Y. Zhang, Z. G. Gan, L. Ma et al., Observation of the Super-heavy Nuclide ^{271}Ds . *Chin. Phys. Lett.* **29** (1), 012502 (2012). doi:10.1088/0256-307X/29/1/012502
- [16] Y. T. Oganessian, V. K. Utyonkov, N. D. Kovrizhnykh et al., New isotope ^{286}Mc produced in the $^{243}\text{Am} + ^{48}\text{Ca}$ reaction. *Phys. Rev. C* **106**, 064306 (2022). doi:10.1103/PhysRevC.106.064306
- [17] S. Hofmann, Synthesis of superheavy elements by cold fusion. *Radiochim. Acta* **99**, 405–428 (2011). doi:10.1524/ract.2011.1854
- [18] S. M. Robinson, J. Allender, N. Bridges et al., Recovery of mark-18a (mk-18a) target materials: Program management plan. Tech. rep., Oak Ridge National Lab.(ORNL), Oak Ridge, TN (United States) (2014). doi:10.2172/1159480
- [19] V. K. Utyonkov, N. T. Brewer, Y. T. Oganessian et al., Experiments on the synthesis of superheavy nuclei ^{284}Fl and ^{285}Fl in the $^{239,240}\text{Pu} + ^{48}\text{Ca}$ reactions. *Phys. Rev. C* **92**, 034609 (2015). doi:10.1103/PhysRevC.92.034609
- [20] V. K. Utyonkov, N. T. Brewer, Y. T. Oganessian et al., Neutron-deficient superheavy nuclei obtained in the $^{240}\text{Pu} + ^{48}\text{Ca}$ reaction. *Phys. Rev. C* **97**, 014320 (2018). doi:10.1103/PhysRevC.97.014320
- [21] Y. T. Oganessian, V. K. Utyonkov, D. Ibadullayev et al., Investigation of ^{48}Ca -induced reactions with ^{242}Pu and ^{238}U targets at the jinr superheavy element factory. *Phys. Rev. C* **106**, 024612 (2022). doi:10.1103/PhysRevC.106.024612
- [22] L. Stavsetra, K. E. Gregorich, J. Dvorak et al., Independent verification of element 114 production in the $^{48}\text{Ca} + ^{242}\text{Pu}$ reaction. *Phys. Rev. Lett.* **103**, 132502 (2009). doi:10.1103/PhysRevLett.103.132502

- [23] P. A. Ellison, K. E. Gregorich, J. S. Berryman et al., New superheavy element isotopes: $^{242}\text{Pu}(^{48}\text{Ca}, 5n)^{285}114$. *Phys. Rev. Lett.* **105**, 182701 (2010). doi:10.1103/PhysRevLett.105.182701
- [24] J. M. Gates, C. E. Düllmann, M. Schädel et al., First superheavy element experiments at the GSI recoil separator TASCA: The production and decay of element 114 in the $^{244}\text{Pu}(^{48}\text{Ca}, 3-4n)$ reaction. *Phys. Rev. C* **83**, 054618 (2011). doi:10.1103/PhysRevC.83.054618
- [25] T. Sikkeland, A. Ghiorso, M. J. Nurmi, Analysis of excitation functions in $\text{Cm}(C, xn)\text{No}$ reactions. *Phys. Rev.* **172**, 1232–1238 (1968). doi:10.1103/PhysRev.172.1232
- [26] M. Murakami, S. Goto, H. Murayama et al., Excitation functions for production of rf isotopes in the $^{248}\text{Cm} + ^{18}\text{O}$ reaction. *Phys. Rev. C* **88**, 024618 (2013). doi:10.1103/PhysRevC.88.024618
- [27] Y. Nagame, M. Asai, H. Haba et al., Status and prospects of heavy element nuclear chemistry research at jaeri. *J. Nucl. Radiochem. Sci.* **3** (1), 129 (2002). doi:10.14494/jnrs2000.3.129
- [28] H. Haba, M. Huang, D. Kaji et al., Production of ^{262}Db in the $^{248}\text{Cm}(^{19}\text{F}, 5n)^{262}\text{Db}$ reaction and decay properties of ^{262}Db and ^{258}Lr . *Phys. Rev. C* **89**, 024618 (2014). doi:10.1103/PhysRevC.89.024618
- [29] H. Haba, D. Kaji, Y. Kudou et al., Production of ^{265}Sg in the $^{248}\text{Cm}(^{22}\text{Ne}, 5n)^{265}\text{Sg}$ reaction and decay properties of two isomeric states in ^{265}Sg . *Phys. Rev. C* **85**, 024611 (2012). doi:10.1103/PhysRevC.85.024611
- [30] J. Dvorak, W. Brühlle, M. Chelnokov et al., Observation of the $3n$ evaporation channel in the complete hot-fusion reaction $^{26}\text{Mg} + ^{248}\text{Cm}$ leading to the new superheavy nuclide ^{271}Hs . *Phys. Rev. Lett.* **100**, 132503 (2008). doi:10.1103/PhysRevLett.100.132503
- [31] Y. T. Oganessian, V. K. Utyonkov, Y. V. Lobanov et al., Measurements of cross sections for the fusion-evaporation reactions $^{244}\text{Pu}(^{48}\text{Ca}, xn)^{292-x}114$ and $^{245}\text{Cm}(^{48}\text{Ca}, xn)^{293-x}116$. *Phys. Rev. C* **69** (5), 054607 (2004). doi:10.1103/PhysRevC.69.054607
- [32] Y. T. Oganessian, V. K. Utyonkov, Y. V. Lobanov et al., Measurements of cross sections and decay properties of the isotopes of elements 112, 114, and 116 produced in the fusion reactions $^{233,238}\text{U}$, ^{242}Pu , and $^{248}\text{Cm} + ^{48}\text{Ca}$. *Phys. Rev. C* **70** (6), 064609 (2004). doi:10.1103/PhysRevC.70.064609
- [33] F. P. Heßberger, D. Ackermann, Some critical remarks on a sequence of events interpreted to possibly originate from a decay chain of an element 120 isotope. *Eur. Phys. J. A* **53** (6), 1–9 (2017). doi:10.1140/epja/i2017-12307-5
- [34] D. Hartanto, D. Chandler, J. W. Bae et al., ^{252}Cf production at the high flux isotope reactor: Nuclear data selection and leu conversion impacts, Tech. rep., Oak Ridge National Laboratory (ORNL), Oak Ridge, TN (United States) (2023).
- [35] M. Tanaka, P. Brionnet, M. Du et al., Probing optimal reaction energy for synthesis of element 119 from $^{51}\text{V} + ^{248}\text{Cm}$ reaction with quasielastic barrier distribution measurement. *J. Phys. Soc. Jpn.* **91** (8), 084201 (2022). doi:10.7566/JPSJ.91.084201
- [36] K. Siwek-Wilczyńska, T. Cap, M. Kowal et al., Predictions of the fusion-by-diffusion model for the synthesis cross sections of $Z = 114$ – 120 elements based on macroscopic-microscopic fission barriers. *Phys. Rev. C* **86**, 014611 (2012). doi:10.1103/PhysRevC.86.014611
- [37] L. Liu, C. W. Shen, Q. F. Li et al., Residue cross sections of ^{50}Ti -induced fusion reactions based on the two-step model. *Eur. Phys. J. A* **52**, 35–39 (2016). doi:10.1140/epja/i2016-16035-0
- [38] C. W. Shen, Y. Abe, D. Boilley et al., Isospin dependence of reactions $^{48}\text{Ca} + ^{243-251}\text{Bk}$. *Int. J. Mod. Phys. E* **17**, 66–79 (2008). doi:10.1142/S0218301308011768
- [39] D. Boilley, Y. Abe, B. Cauchois et al., Elimination of fast variables and initial slip: a new mechanism for fusion hindrance in heavy-ion collisions. *J. Phys. G: Nucl. Part. Phys* **46** (11), 115102 (2019). doi:10.1088/1361-6471/ab11ef
- [40] V. Zagrebaev, W. Greiner, Cross sections for the production of superheavy nuclei. *Nucl. Phys. A* **944**, 257–307 (2015). doi:10.1016/j.nuclphysa.2015.02.010
- [41] S. Amano, Y. Aritomo, M. Ohta, Dynamical mechanism of fusion hindrance in heavy ion collisions. *Phys. Rev. C* **108**, 014612 (2023). doi:10.1103/PhysRevC.108.014612
- [42] Y. H. Zhang, G. Zhang, J. J. Li et al., Production cross sections of $^{243-248}\text{No}$ isotopes in fusion reactions. *Phys. Rev. C* **106**, 014625 (2022). doi:10.1103/PhysRevC.106.014625
- [43] N. Wang, Z. Li, X. Wu, Improved quantum molecular dynamics model and its applications to fusion reaction near barrier. *Phys. Rev. C* **65**, 064608 (2002). doi:10.1103/PhysRevC.65.064608
- [44] X. X. Sun, L. Guo, Microscopic study of the hot-fusion reaction $^{48}\text{Ca} + ^{238}\text{U}$ with the constraints from time-dependent Hartree-Fock theory. *Phys. Rev. C* **107**, 064609 (2023). doi:10.1103/PhysRevC.107.064609
- [45] R. Gumbel, C. Ross, A. S. Umar, Role of isospin composition in low-energy nuclear fusion. *Phys. Rev. C* **108**, L051602 (2023). doi:10.1103/PhysRevC.108.L051602
- [46] A. S. Umar, V. E. Oberacker, J. A. Maruhn et al., Entrance channel dynamics of hot and cold fusion reactions leading to superheavy elements. *Phys. Rev. C* **81**, 064607 (2010). doi:10.1103/PhysRevC.81.064607
- [47] K. Sekizawa, K. Hagino, Time-dependent Hartree-Fock plus Langevin approach for hot fusion reactions to synthesize the $Z = 120$ superheavy element. *Phys. Rev. C* **99**, 051602(R) (2019). doi:10.1103/PhysRevC.99.051602
- [48] L. L. Zhou, J. J. Cai, L. Q. Li et al., Fusion enhancement in the collisions with ^{44}Ca beams and the production of neutron-deficient $^{245-250}\text{Lr}$ isotopes. *Phys. Rev. C* **109**, 024606 (2024). doi:10.1103/PhysRevC.109.024606
- [49] L. Guo, C. W. Shen, C. Yu et al., Isotopic trends of quasifission and fusion-fission in the reactions $^{48}\text{Ca} + ^{239,244}\text{Pu}$. *Phys. Rev. C* **98**, 064609 (2018). doi:10.1103/PhysRevC.98.064609
- [50] N. Wang, E. G. Zhao, W. Scheid et al., Theoretical study of the synthesis of superheavy nuclei with $Z=119$ and 120 in heavy-ion reactions with trans-uranium targets. *Phys. Rev. C* **85**, 041601 (2012). doi:10.1103/PhysRevC.85.041601
- [51] X. J. Bao, Possibility to produce $^{293,295,296}\text{Og}$ in the reactions $^{48}\text{Ca} + ^{249,250,251}\text{Cf}$. *Phys. Rev. C* **100**, 011601 (2019). doi:10.1103/PhysRevC.100.011601
- [52] L. Zhu, Law of optimal incident energy for synthesizing superheavy elements in hot fusion reactions. *Phys. Rev. Res.* **5**, L022030 (2023). doi:10.1103/PhysRevResearch.5.L022030
- [53] L. Zhu, J. Su, F. S. Zhang, Influence of the neutron numbers of projectile and target on the evaporation residue cross sections in hot fusion reactions. *Phys. Rev. C* **93**, 064610 (2016). doi:10.1103/PhysRevC.93.064610
- [54] S. H. Zhu, T. L. Zhao, X. J. Bao, Systematic study of the synthesis of heavy and superheavy nuclei in ^{48}Ca -induced fusion-evaporation reactions. *Nucl. Sci. Tech.* **35**, 124 (2024). doi:10.1007/s41365-024-01483-5
- [55] J. J. Li, C. Li, G. Zhang et al., Theoretical study on production of unknown neutron-deficient $^{280-283}\text{Fl}$ and neutron-rich $^{290-292}\text{Fl}$ isotopes by fusion reactions. *Phys. Rev. C* **98**,

- 014626 (2018). doi:10.1103/PhysRevC.98.014626
- [56] M. H. Zhang, Y. H. Zhang, Y. Zou et al., Predictions of synthesizing elements with $Z = 119$ and 120 in fusion reactions. *Phys. Rev. C* **109**, 014622 (2024). doi:10.1103/PhysRevC.109.014622
- [57] J. J. Li, N. Tang, Y. H. Zhang et al., Progress on production cross-sections of unknown nuclei in fusion evaporation reactions and multinucleon transfer reactions. *Int. J. Mod. Phys. E* **32** (01), 2330002 (2023). doi:10.1142/S0218301323300023
- [58] A. Nasirov, B. Kayumov, Optimal colliding energy for the synthesis of a superheavy element with $Z = 119$. *Phys. Rev. C* **109**, 024613 (2024). doi:10.1103/PhysRevC.109.024613
- [59] S. Madhu, H. C. Manjunatha, N. Sowmya et al., Cr-induced fusion reactions to synthesize superheavy elements. *Nucl. Sci. Tech.* **35**, 90 (2024). doi:10.1007/s41365-024-01449-7
- [60] L. Q. Li, G. Zhang, F. S. Zhang, Production of unknown FI isotopes in proton evaporation channels within the dinuclear system model. *Phys. Rev. C* **106**, 024601 (2022). doi:10.1103/PhysRevC.106.024601
- [61] L. Zhu, W. J. Xie, F. S. Zhang, Production cross sections of superheavy elements $Z = 119$ and 120 in hot fusion reactions. *Phys. Rev. C* **89**, 024615 (2014). doi:10.1103/PhysRevC.89.024615
- [62] X. J. Bao, Y. Gao, J. Q. Li et al., Isotopic dependence of superheavy nuclear production in hot fusion reactions. *Phys. Rev. C* **92**, 034612 (2015). doi:10.1103/PhysRevC.92.034612
- [63] G. G. Adamian, N. V. Antonenko, W. Scheid, Isotopic trends in the production of superheavy nuclei in cold fusion reactions. *Phys. Rev. C* **69**, 011601 (2004). doi:10.1103/PhysRevC.69.011601
- [64] J. Khuyagbaatar, A. Yakushev, C. E. Düllmann et al., Search for elements 119 and 120. *Phys. Rev. C* **102**, 064602 (2020). doi:10.1103/PhysRevC.102.064602
- [65] V. I. Zagrebaev, Synthesis of superheavy nuclei: Nucleon collectivization as a mechanism for compound nucleus formation. *Phys. Rev. C* **64**, 034606 (2001). doi:10.1103/PhysRevC.64.034606
- [66] A. S. Zubov, G. G. Adamian, N. V. Antonenko et al., Survival probability of superheavy nuclei. *Phys. Rev. C* **65**, 024308 (2002). doi:10.1103/PhysRevC.65.024308
- [67] M. H. Zhang, Y. H. Zhang, Y. Zou et al., Possibilities for the synthesis of superheavy element $Z = 121$ in fusion reactions. *Nucl. Sci. Tech.* **35**, 95 (2024). doi:10.1007/s41365-024-01452-y
- [68] W. D. Myers, W. J. Swiatecki, Nuclear masses and deformations. *Nucl. Phys.* **81** (1), 1–60 (1966). doi:10.1016/0029-5582(66)90639-0
- [69] C. Y. Wong, Interaction barrier in charged-particle nuclear reactions. *Phys. Rev. Lett.* **31**, 766–769 (1973). doi:10.1103/PhysRevLett.31.766
- [70] G. G. Adamian, N. V. Antonenko, R. V. Jolos et al., Effective nucleus-nucleus potential for calculation of potential energy of a dinuclear system. *Int. J. Mod. Phys. E* **5**, 191–216 (1996). doi:10.1142/S0218301396000098
- [71] Z. Ahmed, Tunnelling through the morse barrier. *Phys. Lett. A* **157**, 1–5 (1991). doi:10.1016/0375-9601(91)90399-S
- [72] V. Y. Denisov, Expression for the heavy-ion fusion cross section. *Phys. Rev. C* **107**, 054618 (2023). doi:10.1103/PhysRevC.107.054618
- [73] S. Rana, R. Kumar, S. Patra et al., Fusion dynamics of astrophysical reactions using different transmission coefficients. *Eur. Phys. J. A* **58** (12), 241 (2022). doi:10.1140/epja/s10050-022-00893-6
- [74] B. Wang, K. Wen, W. J. Zhao et al., Systematics of capture and fusion dynamics in heavy-ion collisions. *At. Data Nucl. Data Tables* **114**, 281–370 (2017). doi:10.1016/j.adt.2016.06.003
- [75] J. Q. Li, G. Wolschin, Distribution of the dissipated angular momentum in heavy-ion collisions. *Phys. Rev. C* **27**, 590–601 (1983). doi:10.1103/PhysRevC.27.590
- [76] M. H. Zhang, Y. Zou, M. C. Wang et al., Possibility of reaching the predicted center of the “island of stability” via the radioactive beam-induced fusion reactions. *Nucl. Sci. Tech.* **35**, 161 (2024). doi:10.1007/s41365-024-01542-x
- [77] S. Ayik, B. Schürmann, W. Nörenberg, Microscopic transport theory of heavy-ion collisions. *Z. Phys. A* **277** (3), 299–310 (1976). doi:10.1007/BF01415605
- [78] G. G. Adamian, N. V. Antonenko, W. Scheid, Characteristics of quasifission products within the dinuclear system model. *Phys. Rev. C* **68**, 034601 (2003). doi:10.1103/PhysRevC.68.034601
- [79] J. D. Jackson, A schematic model for (p, xn) cross sections in heavy elements. *Can. J. Phys.* **34**, 767–779 (1956). doi:10.1139/p56-087
- [80] V. Weisskopf, Statistics and Nuclear Reactions. *Phys. Rev.* **52**, 295–303 (1937). doi:10.1103/PhysRev.52.295
- [81] N. Bohr, J. A. Wheeler, The mechanism of nuclear fission. *Phys. Rev.* **56**, 426–450 (1939). doi:10.1103/PhysRev.56.426
- [82] L. Zhu, Selection of projectiles for producing trans-uranium nuclei in transfer reactions within the improved dinuclear system model. *J. Phys. G: Nucl. Part. Phys.* **47**, 065107 (2020). doi:10.1088/1361-6471/ab871f
- [83] W. F. Li, Z. Z. Wang, H. S. Xu et al., Odd–Even Effects of the Survival Probability for Superheavy Compound Nuclei. *Chin. Phys. Lett.* **21**, 636 (2004). doi:10.1088/0256-307X/21/4/013
- [84] C. J. Xia, B. X. Sun, E. G. Zhao et al., Systematic study of survival probability of excited superheavy nuclei. *Sci. China Phys. Mech. Astron.* **54**, 109–113 (2011). doi:10.1007/s11433-011-4438-2
- [85] H. Lü, D. Boilley, Y. Abe et al., Synthesis of superheavy elements: Uncertainty analysis to improve the predictive power of reaction models. *Phys. Rev. C* **94**, 034616 (2016). doi:10.1103/PhysRevC.94.034616
- [86] J. A. Sheikh, W. Nazarewicz, J. C. Pei, Systematic study of fission barriers of excited superheavy nuclei. *Phys. Rev. C* **80**, 011302(R) (2009). doi:10.1103/PhysRevC.80.011302
- [87] K. H. Schmidt, W. Morawek, The conditions for the synthesis of heavy nuclei. *Rep. Prog. Phys.* **54** (7), 949 (1991). doi:10.1088/0034-4885/54/7/002